LIMNOLOGY and OCEANOGRAPHY

ASLO

Limnol. Oceanogr. 9999, , 1–15

doi: 10.1002/lno.11013

Assessing the severe eutrophication status and spatial trend in the coastal waters of Zhejiang Province (China)

Q. Jiang,[1] J. He,[1] J. Wu,[1] X. Hu,[2,3] G. Ye,[1*] G. Christakos[1,4*]

[1]Institute of Islands and Coastal Ecosystems, Ocean College, Zhejiang University, Zhoushan, China
[2]State Key Laboratory of Organic Geochemistry, Guangzhou Institute of Geochemistry, Chinese Academy of Sciences, Guangzhou, China
[3]University of the Chinese Academy of Science, Beijing, China
[4]Department of Geography, San Diego State University, San Diego, California

Abstract

The eutrophication of the coastal waters of Zhejiang Province has become one of the main contamination threats to the region's coastal marine ecosystems. Accordingly, the comprehensive characterization of the eutrophication status in terms of improved quantitative methods is valuable for local risk assessment and policy making. A novelty of this work is that the spatial distributions of chemical oxygen demand, dissolved inorganic nitrogen, and dissolved inorganic phosphorus were estimated across space by the Bayesian maximum entropy (BME) method. The BME estimates were found to have the best cross-validation performance compared to ordinary kriging and inverse distance weighted techniques. Based on the BME maps, it was found that about 25.95%, 19.18%, 20.53%, and 34.34% of these coastal waters were oligotrophic, mesotrophic, eutrophic, and hypereutrophic. Another novelty of the present work is that comprehensive stochastic site indicators (SSI) were introduced in the quantitative characterization of the eutrophication risk in the Zhejiang coastal waters under conditions of in situ uncertainty. The results showed that the level of the eutrophication index (EI) increased almost linearly with increasing threshold values; and that 71%, 51%, and 19% of coastal locations separated by various spatial lags experience considerable mesotrophic, eutrophic, and hypereutrophic risks, respectively. The average EI values over the subregions of the Zhejiang coastal waters graded as "oligotrophic or higher," "eutrophic or higher," and "hypereutrophic" were about 11.14, 14.28, and 25.34, respectively. Our results also revealed that the joint eutrophication strength between coastal locations in the Zhejiang region was consistently greater than the combined strength of independent eutrophications at these locations (we termed this situation "positive quadrant eutrophication dependency"). It was found that a critical eutrophication threshold $\zeta_{cr} \approx 8.38$ exists so that below ζ_{cr} the spatial eutrophication dependency in the Zhejiang coastal waters increases with ζ, whereas above ζ_{cr} the opposite is true. Moreover, the eutrophication dependency decreases as the separation distance $\delta\mathbf{s}$ increases. Interestingly, at distances $\delta\mathbf{s}$ smaller than a critical distance $\delta\mathbf{s}_{cr} \approx 15$ km, the eutrophication locations are concentrated in the coastal waters of the Zhejiang province rather than being dispersed (this observation holds even for large thresholds ζ). Elasticity analysis of eutrophication indicators offered a quantitative measure of the excess eutrophication change in the Zhejiang coastal waters caused by a threshold change (the larger the elasticity is, the more sensitive eutrophication is to threshold changes). The above findings can contribute to an improved understanding of seawater quality and provide a practical approach for the identification of critical coastal water regions.

Eutrophication is a type of contamination initially defined as the increase of nutritive substances in a lake (Naumann 1919; Hutchinson 1967), was subsequently adopted in marine waters to characterize water enrichment in nutrients (particularly nitrogen and phosphorus) that leads to increased algae growth (Postma 1966; Vollenweider 1992). Eutrophication of coastal waters can directly and indirectly threaten marine ecosystems with various adverse effects, such as dissolved oxygen consumption, degraded water quality, and changes in species compositions (Heip 1995; Smith 2006; Xiao et al. 2007; Liu et al. 2015). With the rapid economic development of coastal areas in China, eutrophication in marine waters became more severe in coastal regions with high population densities and industrial activities. The last two

*Correspondence: gqy@zju.edu.cn; gchristakos@zju.edu.cn

Additional Supporting Information may be found in the online version of this article.

characteristics result to an increasing flow of anthropogenic nutrients into rivers and accumulation in estuaries and harbors (Chen et al. 2016; Kong et al. 2017; Zhang et al. 2017). Assessment of the eutrophication status is indispensable for environmental conservation management and policy making purposes.

Multiple statistical methods have been used to assess eutrophication, including correlation and regression analysis (Nikolaidis et al. 2006), principal component analysis (PCA; Primpas et al. 2010), and cluster analysis (CA; Lundberg et al. 2009). These data analysis methods and the relevant eutrophication indices rely mainly on the discrete sampling of sites with many water quality parameters such as chemical oxygen demand, dissolved oxygen, nitrogen, phosphorous, and phytoplankton biomass. Although considerable uncertainty may exist for the entire study region, field sampling is often costly and sparsely distributed. Spatial interpolation methods (e.g., inverse distance weighted, and kriging methods), which can generate predictive nutrient maps throughout the study area, have proved very useful tools in the study of coastal marine eutrophication (Kitsiou et al. 2000; Liu et al. 2014; Ren et al. 2016).

This work recognizes the importance of accurate seawater quality mapping in the effective eutrophication assessment and control of the coastal regions in China. This mapping is based on datasets with considerable uncertainty that can affect eutrophication assessment. Accordingly, the Bayesian maximum entropy method of geostatistics will be used to study the severely contaminated by eutrophication coastal waters of Zhejiang province. This method will allow the assimilation of various data sources under conditions of uncertainty, and will generate accurate seawater quality maps across space. Another novelty of the present work is that stochastic site indicators (SSI) will be calculated and used to improve the quantitatively characterization of the eutrophication risk in the Zhejiang coastal waters.

Materials and methods

Study area and data sources

The study region covers an area of 44.4 thousand km^2 (27.0°–31.0°N, 120.4°–123.5°E) of Zhejiang coastal waters along East China Sea. This region was selected according to administrative division procedures (Fig. 1). The study region is located near the Yangtze River and Qiantang River estuaries with developed shipping industry and fishery. Large amounts of anthropogenic nutrients flow into this area, resulting in severe eutrophication, frequent red tides, and deterioration of water quality. As a result, serious concerns have been expressed by both the public and the government. In the present study, samples at 116 monitoring sites during August 2015 were downloaded from China Marine Environmental Monitoring site (www.chmem.cn). Another 205 samples were collected during the same period by the Marine Monitoring and Forecasting Center of Zhejiang Province. Monitoring indicators include many water quality attributes, such as pH, chemical oxygen demand (COD), dissolved inorganic nitrogen (DIN, the sum value of NO_2-N, NO_3-N, and NH_3-N), and dissolved inorganic phosphorus (DIP). The analysis methods for parameter concentration assessment followed China's national standards, GB17378-2007 (www.soa.gov.cn). In this work, we focused on COD, DIN, and DIP, because they are important eutrophication indicators related to algal blooms and the water ecological cycle.

Spatial mapping of seawater quality indices by Bayesian maximum entropy

The Bayesian maximum entropy (BME) method proposed by Christakos (1990, 2000) was used in this work to map the spatial distributions of water quality attribute concentrations (COD, DIN, and DIP) in the study area. BME has been applied successfully in many fields including air pollution (Yu et al. 2011; Yang and Christakos 2015), soil pollution (Modis et al. 2013), and fecal pollution (Coulliette et al. 2009). In the BME modeling context, a water quality attribute is represented as the spatial random field $X(\boldsymbol{s})$, where the vector $\boldsymbol{s} = (s_1, s_2)$ denotes spatial location. Then, BME generates accurate estimates of water quality attribute concentrations by assimilating knowledge bases (KB) from different sources, such as the core or general (G) and the site-specific (S) KB (as described, e.g., in He and Kolovos 2017). The basic BME equations are.

$$\int d\mathbf{x}(\boldsymbol{g}-\overline{\mathbf{g}})f_{\mathrm{G}} = 0, \quad (1)$$

$$\int d\mathbf{x}\xi_{\mathrm{S}} - af_{\mathrm{K}} = 0, \quad (2)$$

where the bar denotes average value, the $\mathbf{x}$ represents realizations of the concentrations of a water quality attribute $X(\boldsymbol{s})$ (COD, DIN, and DIP) with probability of occurrence determined by the corresponding probability density function (pdf) of the three attributes, the $\boldsymbol{g}$ is a vector function describing the components of the available G-KB, $\xi_{\boldsymbol{s}}$ denotes the available S-KB, f_{G} and f_{K} denote the pdf describing probabilistically the prior (G) KB and the posterior (combined G and S) KB, respectively, and a is a normalization parameters (more technical details can be found in the relevant BME literature).

In this work, the G-KB included the theoretical mean and covariance models of the COD, DIN, and DIP distributions (the theoretical models are shown in Supporting Information Fig. S1 together with the empirical correlation values). And the S-KB consisted of (1) the national sample data mentioned earlier, which was treated as hard data, and (2) the soft data represented by Gaussian probability functions with means and variances obtained by linear regression between the national and the regional samples. Data processing and the BME method were implemented in terms of, respectively, the software R-version 3.3.3 and the Spatiotemporal Epistemic Knowledge Synthesis Graphical User Interface library (SEKS-GUI, Yu et al. 2007).

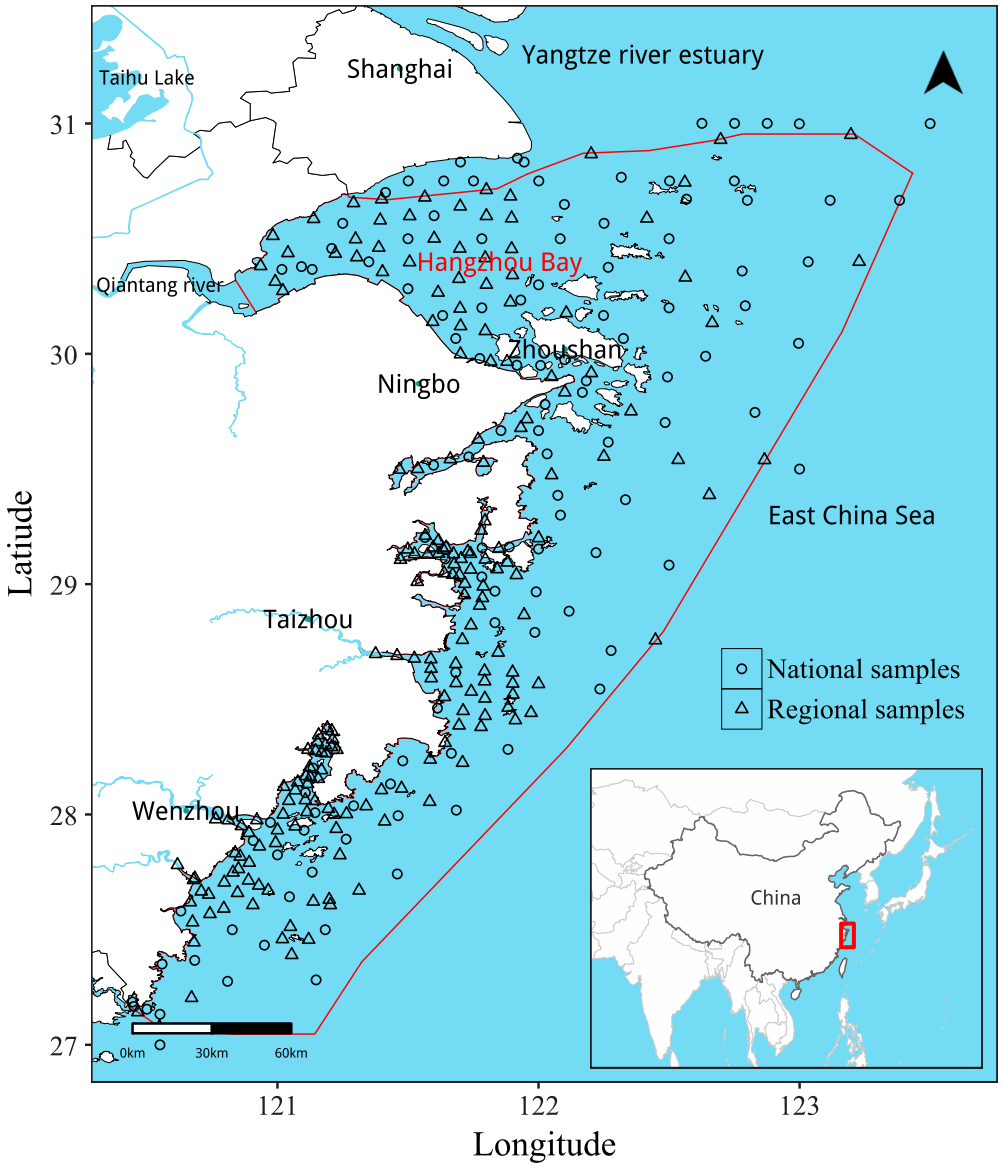

Fig. 1. Study region (coastal waters of Zhejiang province) and sample locations.

To evaluate the quality of the COD, DIN, and DIP maps obtained by the BME method, the ordinary kriging (OK) and the inverse distance weighted (IDW) mapping techniques were also used for comparison purposes. The cross-validation procedure comparing the results of these techniques: (1) divided the dataset into a training set (70% of the samples) and a test set (30% of the samples), and (2) involved two accuracy indicators, the mean absolute error (MAE) and the root mean square error (RMSE); see below, section on Results and Discussion.

Eutrophication index

The eutrophication index (EI) is a critical eutrophication level that defines the trophic eutrophication status. This index, which is widely used by the State Oceanic Administrative of China (SOA), has been implemented in many earlier studies (e.g., Quan et al. 2005; Yu et al. 2013; Zhang et al. 2017). Using the COD, DIN, and DIP concentration maps generated by BME over the entire study region, the corresponding EI was calculated by.

$$\mathrm{EI} = \frac{C_{\mathrm{COD}} C_{\mathrm{DIN}} C_{\mathrm{DIP}}}{4500} 10^6, \tag{3}$$

where C_{COD}, C_{DIN}, and C_{DIP} denote, respectively, the COD, DIN, and DIP concentrations of surface seawater; and EI is a unitless indicator used in the classification of the eutrophication level. The water body is considered oligotrophic when EI < 1, mesotrophic when 1 ≤ EI ≤ 3, eutrophic when 3 < EI ≤ 9, and hypereutrophic when EI > 9.

Table 1. One-point and two-point SSI.

One-point SSI	Definition	Interpretation
Relative area of excess contamination (RAEC)	$R_{\mathrm{EI}}(\zeta) = \overline{I_{\mathrm{EI}}(\boldsymbol{s},\zeta)}$	Areal fraction where ζ-exceeding eutrophication incidences occur
Mean excess contamination (MEC)	$P^{D}_{\mathrm{EI}}(\zeta) = \overline{\mathrm{EI}(\boldsymbol{s}) I_{\mathrm{EI}}(\boldsymbol{s},\zeta)}$	Average ζ-exceeding eutrophication value over a region
Mean excess differential contamination (MEDC)	$L^{D}_{\mathrm{EI}}(\zeta) = \overline{[\mathrm{EI}(\boldsymbol{s})-\zeta] I_{\mathrm{EI}}(\boldsymbol{s},\zeta)}$	Average ζ-differential EI value over a region
Conditional MEC (CMEC)	$P^{\Theta}_{\mathrm{EI}}(\zeta) = \overline{\mathrm{EI}(\boldsymbol{s}) \mid \mathrm{EI}(\boldsymbol{s}) \geq \zeta}$	Conditional ζ-exceeding EI value over a contaminated subregion
Contaminant indicator dispersion (CID)	$\Psi_{EI} = \frac{\overline{L^{D}_{\mathrm{EI}}(\zeta)}}{\overline{\mathrm{EI}}}$	Average ζ-differential EI spread over a region
Two-point SSI	**Definition ($\delta s = s' - s$)**	**Interpretation**
Noncentered indicator covariance (NIC)	$c_{\mathrm{I}}(\delta\boldsymbol{s};\zeta) = \overline{I_{\mathrm{EI}}(\boldsymbol{s},\zeta) I_{\mathrm{EI}}(\boldsymbol{s}',\zeta)}$	Covariation strength of joint eutrophication incidences across space
Centered indicator covariance (CIC)	$\tilde{c}_{\mathrm{I}}(\delta\boldsymbol{s};\zeta) = c_{\mathrm{I}}(\delta\boldsymbol{s};\zeta) - R^2_{\mathrm{EI}}(\zeta)$	Covariation strength of joint eutrophication incidences across space vs. strength of independent eutrophication incidences across space
Contaminant interaction ratio (CIR)	$G_{\mathrm{EI}}(\delta\boldsymbol{s},\zeta) = \frac{c_{\mathrm{I}}(\delta\boldsymbol{s};\zeta)}{2R_{\mathrm{EI}}(\zeta) - c_{\mathrm{I}}(\delta\boldsymbol{s};\zeta)}$	Covariation strength of joint eutrophication incidences across space vs. covariation strength of alternate eutrophication incidences across space
Noncentered excess covariance (NEC)	$P^{D}_{\mathrm{EI}}(\delta\boldsymbol{s};\zeta) = \overline{\mathrm{EI}(\boldsymbol{s})\mathrm{EI}(\boldsymbol{s}') I_{\mathrm{EI}}(\boldsymbol{s},\zeta) I_{\mathrm{EI}}(\boldsymbol{s}',\zeta)}$	Spatial correlation between ζ-exceeding EI values
Excess differential covariance (EDC)	$L^{D}_{\mathrm{EI}}(\delta\boldsymbol{s};\zeta) = \overline{[\mathrm{EI}(\boldsymbol{s})-\zeta][\mathrm{EI}(\boldsymbol{s}')-\zeta] I_{\mathrm{EI}}(\boldsymbol{s},\zeta) I_{\mathrm{EI}}(\boldsymbol{s}',\zeta)}$	Spatial correlation between differential EI values
Conditional excess covariance (CEC)	$P^{\Theta}_{EI}(\delta\boldsymbol{s};\zeta) = \overline{EI(\boldsymbol{s})EI(\boldsymbol{s}') \mid EI(\boldsymbol{s}), EI(\boldsymbol{s}') \geq \zeta}$	Conditional correlation among ζ-exceeding EI values across space

Stochastic site indicators

The stochastic site indicators (SSI) proposed by Christakos and Hristopulos (1996*a*,*b*, 1997) were used in this work to characterize nitrate and phosphate contamination in the coastal waters of Zhejiang province. Let EI($\boldsymbol{s}$) be the random field model representing mathematically the variation of the eutrophication index in the Zhejiang coastal water region denoted as D (in this case, the focus of the BME Eqs. 1, 2 above should be EI($\boldsymbol{s}$)). Then, a binary random field, termed the binary EI characteristic, can be defined in terms of EI($\boldsymbol{s}$) as.

$$I_{\mathrm{EI}}(\boldsymbol{s},\zeta) = \begin{cases} 1 & \mathrm{EI}(\boldsymbol{s}) \geq \zeta \\ 0 & \text{otherwise,} \end{cases} \tag{4}$$

where ζ is a specified threshold (in this work, ζ denotes the EI range), and the $I_{\mathrm{EI}}(\boldsymbol{s}, \zeta)$ offers a spatial characterization of the excess eutrophication index in the study region D (i.e., it focuses on the EI values that exceed the specified ζ). Noticeably, while EI($\boldsymbol{s}$) is a function of the location $\boldsymbol{s}$, the $I_{\mathrm{EI}}(\boldsymbol{s}, \zeta)$ is a function of both $\boldsymbol{s}$ and ζ. The SSI-based eutrophication (contamination) characterization involves the pair {EI($\boldsymbol{s}$), $I_{\mathrm{EI}}(\boldsymbol{s}, \zeta)$}.

The SSI of the EI distribution, including one-point and two-point indicators, are listed in Table 1. Two regional spatial domains were distinguished: the entire Zhejiang coastal region is denoted as D, and its subregion Θ is characterized as the contaminated part D. This means that Θ is defined so that for all locations $\boldsymbol{s} \in \Theta$ it is true that EI($\boldsymbol{s}$) > ζ, and that $\Theta \subset D$. Moreover, for any selected eutrophication threshold ζ, the following quantitative limits and relationships hold,

$$R_{\mathrm{EI}}(\infty) = 0 \leq R_{\mathrm{EI}}(\zeta) \leq R_{\mathrm{EI}}(0) = 1,$$
$$P^{D}_{\mathrm{EI}}(\infty) = 0 \leq P^{D}_{\mathrm{EI}}(\zeta) \leq P^{D}_{\mathrm{EI}}(0) = \overline{\mathrm{EI}(\boldsymbol{s})},$$
$$P^{\Theta}_{\mathrm{EI}}(0) = \overline{\mathrm{EI}(\boldsymbol{s})} \leq P^{\Theta}_{\mathrm{EI}}(\zeta),$$
$$L^{D}_{\mathrm{EI}}(\infty) = 0 \leq L^{D}_{\mathrm{EI}}(\zeta) \leq L^{D}_{\mathrm{EI}}(0) = \overline{\mathrm{EI}(\boldsymbol{s})},$$

as regards the one-point SSI of eutrophication status (Table 1).

The one-point SSI may be assigned more than one interpretations that offer alternative perspectives of the global eutrophication status. The RAEC indicator may be viewed as the probability that a location chosen at random belongs to the contaminated subregion Θ. It may be also seen as the fraction of the region of interest D in which threshold ζ-exceeding eutrophication incidences occur (i.e., RAEC is a topological indicator that focuses on the occurrence of ζ-exceeding eutrophication incidences rather than on the eutrophication

values). On the other hand, the MEC, MEDC and CMEC indicators provide different measures of areal eutrophication values, i.e., they are substantive indicators. In particular, MEC is the average of the EI values exceeding the selected eutrophication threshold ζ over the study region (D). The MEDC calculates the average ζ-differential EI value (i.e., EI – ζ) over the same region, whereas the CMEC is the ζ-exceeding EI averaged over the contaminated subregion (Θ) only. Last, the CID indicator, Ψ_{EI}, measures the average ζ-differential EI spread over the study region. It has convenient analytical expressions in the rather commonly encountered cases that the distribution of the EI follows one of the well-known probability laws. In particular,

$$\Psi_{EI} = \begin{cases} \dfrac{\sigma_{EI}}{\sqrt{\pi \overline{EI}}} & \text{if } EI(\boldsymbol{s}) \sim \text{Gaussian law,} \\ 2G_{EI}\left(\dfrac{\sigma_{EI}}{\sqrt{2\overline{EI}}}\right) - 1 & \text{if } EI(\boldsymbol{s}) \sim \text{Lognormal law,} \\ \dfrac{1}{2} & \text{if } EI(\boldsymbol{s}) \sim \text{Exponential law} \end{cases} \qquad (5a\text{-}c)$$

where G_{EI} denotes the Gaussian probability law, and $\overline{EI(\boldsymbol{s})}$ and σ_{EI} denote, respectively, the spatial mean and the standard deviation of the eutrophication index.

While the one-point (global) SSI in Table 1 are generally functions of the threshold ζ and evaluate global eutrophication averages, spatial relationships or dependencies can be assessed by two-point SSI that are functions of both the ζ and the distance $\delta\mathbf{s} = \mathbf{s}' - \mathbf{s}$ between locations $\mathbf{s}$ and $\mathbf{s}'$ (i.e., the two-point SSI account for the eutrophication direction and its anisotropic features). The two-point SSI, which are also listed in Table 1, take advantage of the useful property that the probability law of the EI($\boldsymbol{s}$) distribution is expressed in terms of the spatial statistics of the corresponding binary characteristic $I_{EI}(\boldsymbol{s}, \zeta)$ distribution of Eq. 4.

The joint occurrence of ζ-exceeding eutrophication incidences at different locations is a considerable ecoregional risk factor. Accordingly, the two-point SSI can be arranged into two main groups: (1) Since a better understanding of the dependence between eutrophication incidences across space is crucial to contamination risk assessment, the NIC, CIC, and CIR indicators have been developed to describe quantitatively this dependence (this is a group of topological indicators, because they focus on the regional distribution of eutrophication incidences rather than on the eutrophication values). (2) The NEC, EDC, and CEC indicators, on the other hand, represent the spatial correlation structure of the eutrophication values associated with these incidences (which is why they are characterized as substantive).

Like the one-point SSI considered above, the two-point SSI too may be assigned alternative interpretations that look at the eutrophication situation from different perspectives. Particularly, a two-point SSI could be interpreted in regional correlation terms as well as in probability terms. In this setting, the NIC indicator, $c_I(\delta\mathbf{s}; \zeta)$, expresses the correlation strength of ζ-exceeding EI incidences in terms of the covariance of the eutrophication characteristic I_{EI}. In probability terms, the NIC assesses the joint probability of eutrophication incidences at both locations $\mathbf{s}$ and $\mathbf{s}' = \mathbf{s} + \delta\mathbf{s}$ (that is, the NIC measures how eutrophication incidences at different locations covary when they both exceed the specified threshold ζ).

The CIC indicator, $\widetilde{c}_I(\delta\mathbf{s};\zeta)$, expresses the covariation strength of ζ-exceeding eutrophication incidences centered around the one-point RAEC indicator. As such, CIC measures how the eutrophication incidences covary across space (i.e., how they behave together when they simultaneously exceed the threshold ζ) compared to how these eutrophication incidences vary in separation (i.e., how they behave when they independently exceed ζ). More precisely, CIC measures the strength of eutrophication dependency across space as the difference of "the joint probability of ζ-exceeding eutrophication at both coastal locations $\mathbf{s}$ and $\mathbf{s}'$" minus the product of "the probability of ζ-exceeding eutrophication at location $\mathbf{s}$" times "the probability of ζ-exceeding eutrophication at location $\mathbf{s}'$."

A useful distinction can be then made as regards the possible ranges of CIC values: (1) If $\widetilde{c}_I(\delta\mathbf{s};\zeta) \geq 0$, the spatial dependency will be termed positive quadrant eutrophication dependency (PQED). PQED occurrence implies that eutrophication incidences at two locations are more closely dependent when they are considered simultaneously than when they are considered independent of each other. Accordingly, the eutrophication incidences at these locations are PQED if the probability that they simultaneously exceed threshold ζ is at least as large as it would be if the incidences were independent. (2) The case $\widetilde{c}_I(\delta\mathbf{s};\zeta) \leq 0$ will be termed a negative quadrant eutrophication dependency (NQED), which implies that eutrophication incidences at two locations are more closely dependent when they are considered separately than when they are considered simultaneously. Accordingly, eutrophication will be characterized as NQED if the probability of simultaneous ζ-exceedance is at most as large as it would be if the incidences were independent.

On the basis of the above distinction, other useful comparisons could be made. If $\widetilde{c}_I(\delta\mathbf{s};\zeta) \geq \widetilde{c}_I(\delta\mathbf{s};\zeta') \geq 0$, the ζ-exceeding eutrophication dependency in a region is more PQED than the ζ'-exceeding dependency. Similarly, if $\widetilde{c}_I(\delta\mathbf{s};\zeta) \geq \widetilde{c}_I(\delta\mathbf{s}';\zeta) \geq 0$, the eutrophication dependency at separation distance $\delta\mathbf{s}$ is more PQED than the dependency at distance $\delta\mathbf{s}'$.

The CIR indicator, $G_{EI}(\delta\mathbf{s}, \zeta)$, compares the covariation strength of different distributions of eutrophication incidences across space. In particular, it compares how the eutrophication incidences at two locations covary when they simultaneously exceed threshold ζ compared to how these eutrophication incidences covary when either one of them exceeds ζ. As such, CIR may be calculated as the probability ratio of joint over alternate ζ-exceeding eutrophication incidences across space.

The substantive NEC indicator, $P_{EI}^{D}(\delta\mathbf{s};\zeta)$, measures the correlation between eutrophication values at locations $\mathbf{s}$ and $\mathbf{s}'$ in

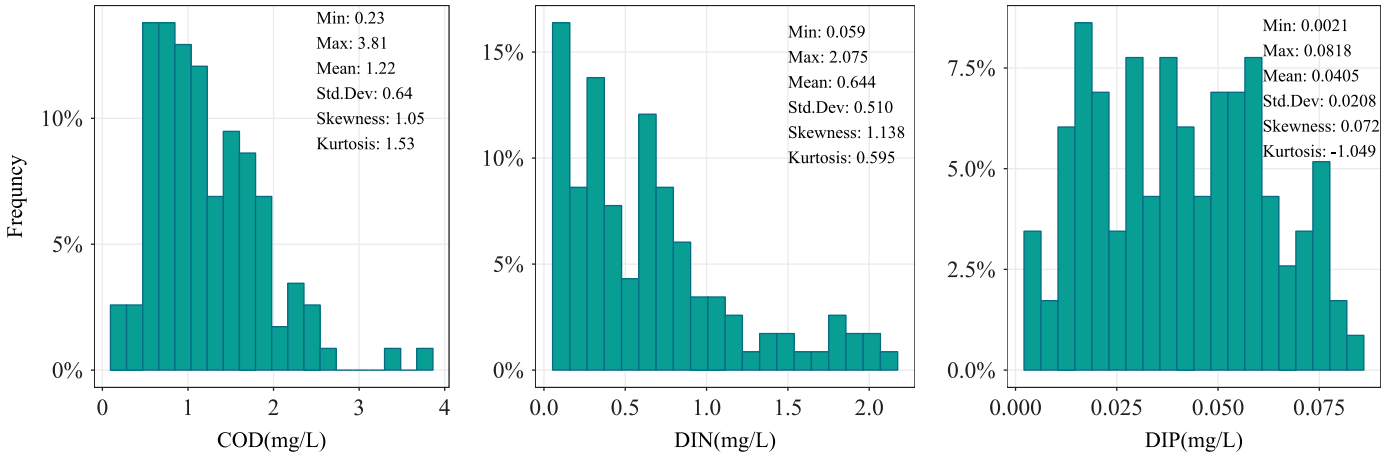

Fig. 2. Descriptive statistics of the COD, DIN, and DIP concentrations in the coastal waters of Zhejiang province.

which EI exceeds the specified threshold. The EDC, $L_{\mathrm{EI}}^{D}(\delta\mathbf{s};\zeta)$, measures the connectivity between ζ-differential eutrophication values (i.e., EI – ζ) between contaminated locations at distance $\delta\mathbf{s} = \mathbf{s}' - \mathbf{s}$ apart. Last, the CEC, $P_{\mathrm{EI}}^{\Theta}(\delta\mathbf{s};\zeta)$, measures the conditional eutrophication variation between locations $\mathbf{s}$ and $\mathbf{s}'$ given that both locations exceed ζ. In this work, the presentation of the practical implementation and numerical results of the two-point SSI in the study of the Zhejiang coastal waters was divided into two parts: the implementation and results of the NIC, CIC, and CIR indicators are presented below, whereas the implementation and results of the NEC, CEC, and EDC indicators are discussed in the Supporting Information section.

Last, an additional water quality indicator was calculated, namely, the contaminant indicator elasticity (CIE) of an eutrophication SSI ($\mathrm{SSI_{EI}}$) to changes in threshold ζ, where SSI may denote any of the indicators of Table 1. The CIE is defined as

$$Q_{\mathrm{SSI}}(\zeta) = \frac{\frac{d\mathrm{SSI_{EI}}(\zeta)}{\mathrm{SSI_{EI}}(\zeta)}}{\frac{d\zeta}{\zeta}}, \tag{6}$$

i.e., the ζ-elasticity of $\mathrm{SSI_{EI}}$ in Eq. 6 is a measure of the responsiveness of $\mathrm{SSI_{EI}}$ to changes in ζ. Hence, Q_{SSI} calculates how fast the $\mathrm{SSI_{EI}}$ changes compared to how fast the environmental threshold changes (or, equivalently, the percent change in $\mathrm{SSI_{EI}}$ caused by an 1% c in ζ). In practice, three possibilities may be considered: if $0 < Q_{\mathrm{SSI}}(\zeta) < 1$, then $\mathrm{SSI_{EI}}$ increases slower than ζ; if $Q_{\mathrm{SSI}}(\zeta) > 1$, then $\mathrm{SSI_{EI}}$ increases faster than ζ; and if $Q_{\mathrm{SSI}}(\zeta) < 0$, then $\mathrm{SSI_{EI}}$ decreases with increasing ζ.

An obvious implication of eutrophication elasticity analysis in practice is that, the larger the elasticity Q_{SSI} of the eutrophication indicator $\mathrm{SSI_{EI}}$ is, the more sensitive the indicator is to environmental threshold changes. For illustration, consider the case of the MEDC eutrophication indicator, i.e., let $\mathrm{SSI_{EI}}(\zeta) = L_{\mathrm{EI}}^{D}(\zeta)$. The corresponding CIE, $Q_{L_{\mathrm{EI}}^{D}}$, measures the percent change of differential eutrophication over the Zhejiang coastal waters per unit ζ change. Hence, if the threshold changes by $d\zeta$, then the MEDC change, $\frac{dL_{\mathrm{EI}}^{D}(\zeta)}{L_{\mathrm{EI}}^{D}(\zeta)}$, will be given by $Q_{L_{\mathrm{EI}}^{D}}(\zeta)\frac{d\zeta}{\zeta}$. Later, we will discuss some more CIE elasticity expressions that are useful in the calculation of $Q_{L_{\mathrm{EI}}^{D}}$ in practice.

Results and discussion

Descriptive statistics

Figure 2 displays the histograms of the COD, DIN, and DIP concentrations at the sampling sites during August 2015. The mean COD, DIN, and DIP concentrations were, respectively, 1.22 mg/L (with a range 0.23–3.81 mg/L), 0.644 mg/L (0.059–2.075 mg/L), and 0.0405 mg/L (0.0021–0.0818 mg/L).

The maximum COD concentration was below the 2$^{\mathrm{nd}}$ grade of water quality standard (GB3097-1997), whereas DIN and DIP were far beyond the 4$^{\mathrm{th}}$ grade. And, the COD and DIN concentrations showed a deviation to left with most values less than 2.0 mg/L and 1.0 mg/L, respectively. Last, the DIP concentrations exhibit a relatively uniform distribution (Kolmogorov–Smirnov test, $p > 0.05$).

Water quality maps and cross-validation results

The COD, DIN, and DIP concentration maps generated by the IDW, OK, and BME methods are presented in Fig. 3. The results show that although considerable local differences exist between the water quality maps generated by the three mapping methods, similar COD, DIN, and DIP distribution trends emerge across space (all spatial maps of the COD, DIN, and DIP concentrations show a global decreasing trend from the coastal estuary to the open sea). The COD concentrations are generally larger than the DIN concentrations, and much larger than the DIP concentrations (all mg/L).

In particular, it is worth-noticing that Hangzhou Bay, where there are many coastal factories and abundant human activities, shows significantly higher nitrate and phosphate concentrations than other areas. Moreover, extremely high

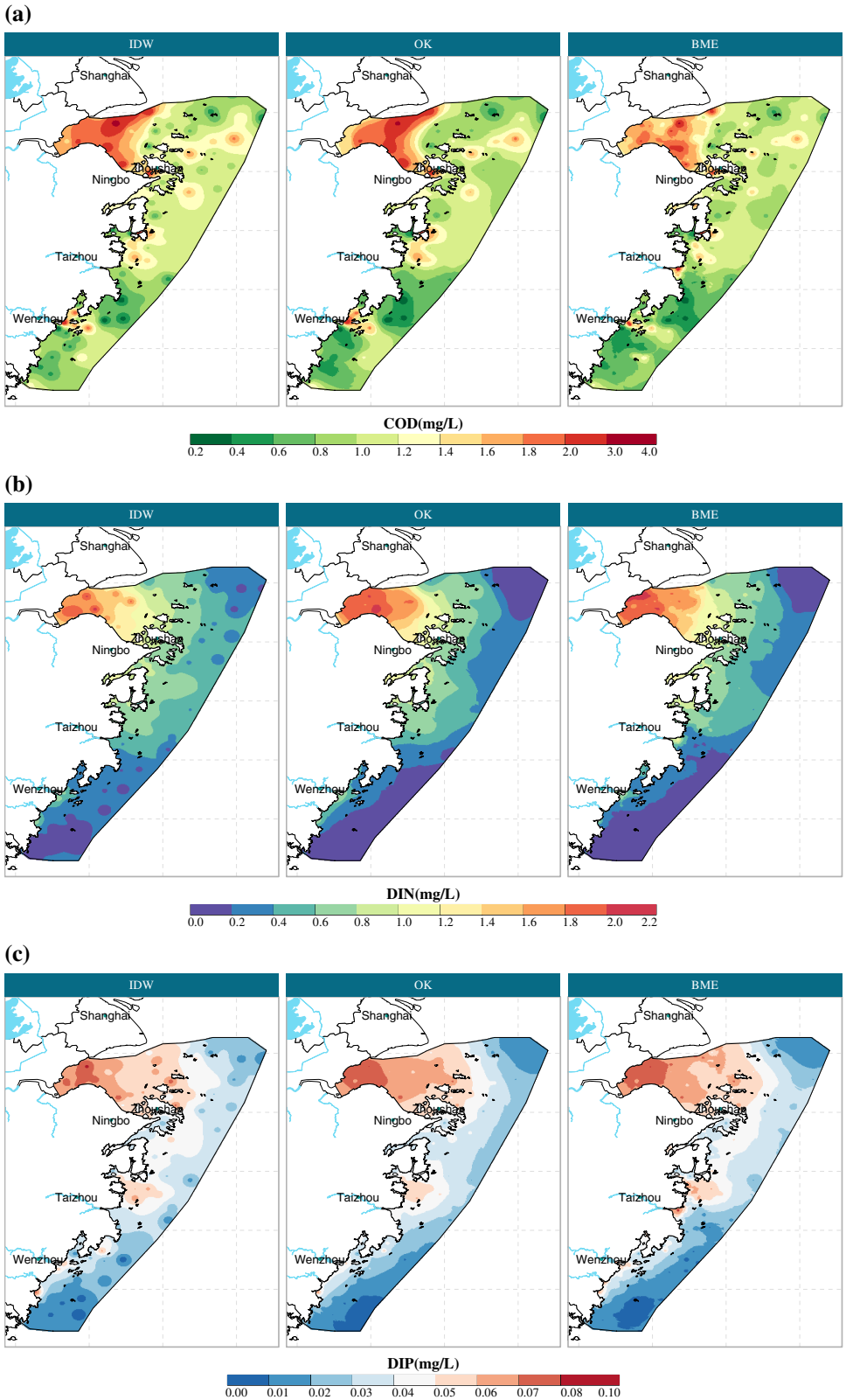

Fig. 3. COD (**a**), DIN (**b**), and DIP (**c**) maps obtained by the IDW, OK, and BME interpolation techniques.

values were found in estuaries characterized by increasing human disturbances and pollutant accumulations from the upstream freshwater. Note that nitrogen and phosphorus levels are generally expected to increase as the original forestland and grassland decline, which is why the original forestland and urban land are often identified as land-uses closely linked to water quality changes. Also, excessive fertilization and land fragmentation contribute significantly to increasing nutrient loads observed in rivers, which, in turn, may increase the extent of coastal water eutrophication. Nutrient maps, such as those in Fig. 3, may also help chose spatial indicators that can identify the most sensitive water quality indicators exhibiting the closest relationship to coastal water eutrophication, and consistently link water quality with key factors like land-use and cover-change. Last, these maps could be very useful in decision-making regarding the optimal choice of spatial monitoring stations.

For comparative analysis purposes, three different interpolation techniques were used in the present study to generate water quality maps in the Zhejiang region (spatial variations of COD, DIN, and DIP concentrations):

a. The IDW technique (e.g., Siu-Nganlam 1983) is the simplest among the three techniques. It is a deterministic interpolator with predefined weights, i.e., ID assigns values to unsampled locations of the Zhejiang coastal waters in terms of a weighted average of concentrations at the sample points with weights proportional to the inverse distances between the interpolated point and each sample point (the effect of the inverse distance weights can be determined ad hoc by varying the power that the inverse distance is raised to). No determination of spatial correlation (covariance) is account for by IDW. Instead, only samples and distance weights are used to derive estimates at unsampled mapping points.
b. The OK technique (e.g., Olea 1999) is a linear interpolator that generates concentration estimates at unsampled locations based on the unbiased minimization of the interpolation error variance (i.e., unlike IDW, OK uses a statistical model). OK calculates spatial correlations between points as a function of their separation distances and uses this calculation to determine the interpolation weights to be applied at these distances. OK assumes a normal (Gaussian) distribution of the COD, DIN, and DIP concentrations. Among the OK advantages over IDW are that OK does not predetermine the form of the interpolation weights, and it provides an assessment of interpolation accuracy in terms of the OK error. Hence, the use of OK is more appropriate than IDW when the data are spatially correlated and/or there is a directional bias (anisotropy) in the data.
c. The BME technique (introduced earlier) is a considerable improvement over the previous two techniques. BME shares the attractive features of OK (it provides an interpolation accuracy assessment etc.), but it is considerably more versatile than OK (and several other types of Kriging, for that matter). Unlike OK, BME makes no restrictive assumptions concerning both the linearity of the interpolator and the normal probability distribution of the samples (i.e., the more general nonlinear interpolators and non-normal probability distributions are automatically incorporated in BME). In addition to the conditional mean-based maps (also provided by OK), BME can produce other kinds of maps, like median and mode-based maps, if more appropriate. Compared to the IDW and OK maps, the BME maps reveal not only the global contamination trends throughout the Zhejiang coastal waters, but they also depict the small-scale variations of COD, DIN, and DIP concentrations. This is possibly due to BME's ability to avoid the limiting assumptions mentioned above and to process information from different sources (in addition to the commonly used hard data, soft information of various types can be also processed by BME).

Table 2. Cross-validation results of the three different interpolation techniques (IDW, OK, and BME).

	COD (mg/L)		DIN (mg/L)		DIP (mg/L)	
	MAE	RMSE	MAE	RMSE	MAE	RMSE
IDW	0.3305	0.4144	0.1593	0.2109	0.0117	0.0141
OK	0.3275	0.4080	0.1063	0.1424	0.0114	0.0140
BME	0.3127	0.3924	0.0836	0.1060	0.0099	0.0119

In this work, the theoretical superiority of BME was tested in computational terms. For illustration, the numerical cross-validation results in Table 2 demonstrated that the BME technique consistently exhibited the best performance among the three techniques, with the lowest mean absolute error (MAE) and root mean square error (RMSE) values for the water quality (COD, DIN, and DIP prediction) tests. Furthermore, point-based cross-validation results (Supporting Information Fig. 2) showed that BME predictions are closer to the actual (in situ) concentration data. Accordingly, the most accurate BME water quality maps were used in subsequent eutrophication assessment and SSI calculations in this work.

Eutrophication assessment and classification maps

Table 3 summarizes the areal percentages of each seawater quality attribute in the Zhejiang coastal waters together with the calculated eutrophication index (EI). The COD concentrations met the seawater quality standards (Supporting Information Table 1) with about 99.3% of the study region being under the 1st grade (COD ≤ 2 mg/L). The region was heavily contaminated by nitrogen and phosphorus, with 43.06% and 32.4% of the study area exceeding the 4th grade ($N > 0.5$ mg/L, and $p > 0.045$ mg/L, respectively). The average EI value was found to be 8.38, with a range from 0.04 to 103.3. According to the EI maps, about 25.95%, 19.18%, 20.53%, and 34.34% of the study region were characterized as oligotrophic,

Table 3. Classification of COD, DIN, and DIP concentrations estimated by BME, and associated EI values. The *q*-statistic was used to test spatial stratified heterogeneity; the *p*-value is the probability of *q*-statistic.

	Percentage of coastal area (%)					Spatial stratified heterogeneity	
	I	II	III	IV	Over IV	*q*-statistic	*p*-value
COD	99.3	0.69	0.01	0	0	0.09	1.9×10^{-9}
DIN	21.42	10.15	11.97	13.39	43.06	0.60	8.2×10^{-10}
DIP	9.34	23.48		34.78	32.4	0.89	1.9×10^{-10}
EI	Oligotrophic	Mesotrophic	Eutrophic	Hypereutrophic		0.59	1.3×10^{-9}
	25.95	19.18	20.53	34.34			

mesotrophic, eutrophic, and hypereutrophic, respectively. It was found that the Zhejiang coastal water area dominated by 1st grade nitrogen concentrations is much larger than the corresponding area dominated by phosphorus concentrations. Nitrogen controls should be recognized in alleviating coastal eutrophication, while both nitrogen and phosphorous loading reduction are required (Howarth and Marino 2006; Conley et al. 2009). Furthermore, we found that the area dominated by 5th grade nitrogen concentrations is two times larger than the area of 4th grade nitrogen concentrations.

The EI classification map of Fig. 4 demarcates the spatial distribution of domains with different eutrophication levels (oligotrophic, mesotrophic, eutrophic, and hypereutrophic). This kind of map is useful for contamination management purposes. It is also noticed that the spatial EI classification pattern in Fig. 4 is similar to the spatial DIN and DIP concentration patterns in Fig. 3, which also exhibited decreasing trends from the estuary to the open sea, and indicated the serious eutrophication status and trend in Hangzhou Bay.

Moreover, the *q*-statistic (Wang et al. 2016) was employed to test the spatial stratified heterogeneity of the classification results. It was calculated by GeoDetector (Wang et al. 2010) and defined as

$$q = 1 - \frac{\sum_{h=1}^{L} N_h \sigma_h^2}{N\sigma^2},$$

where N is the total number of samples, and σ^2 and σ_h^2 are the variances of the entire study region and each sub-region (h = 1, 2, …, L), respectively. In theory, the value of the q-statistic varies within the interval [0,1], and it increases monotonically with increasing stratified heterogeneity. In this study, the q values are 0.09, 0.60, 0.89, and 0.59 for COD, DIN, DIP, and EI, respectively. At the statistical significance level, all p-values are < 0.01 demonstrating a reasonable classification (except for COD with a low q value).

Calculation of eutrophication SSI in the Zhejiang coastal waters

One-point SSI

Based on the maps obtained by the BME method above, valuable information was obtained in terms of the corresponding SSI characterizing eutrophication in the coastal waters of the Zhejiang province. The one-point SSI indicators, i.e., RAEC, MEC, MEDC, and CMEC, were first plotted in Fig. 5a. As is shown in this figure, the RAEC, MEC, and MEDC indicators are all decreasing functions of the threshold ζ, whereas the CMEC indicator is an increasing function of ζ (these SSI offer different local

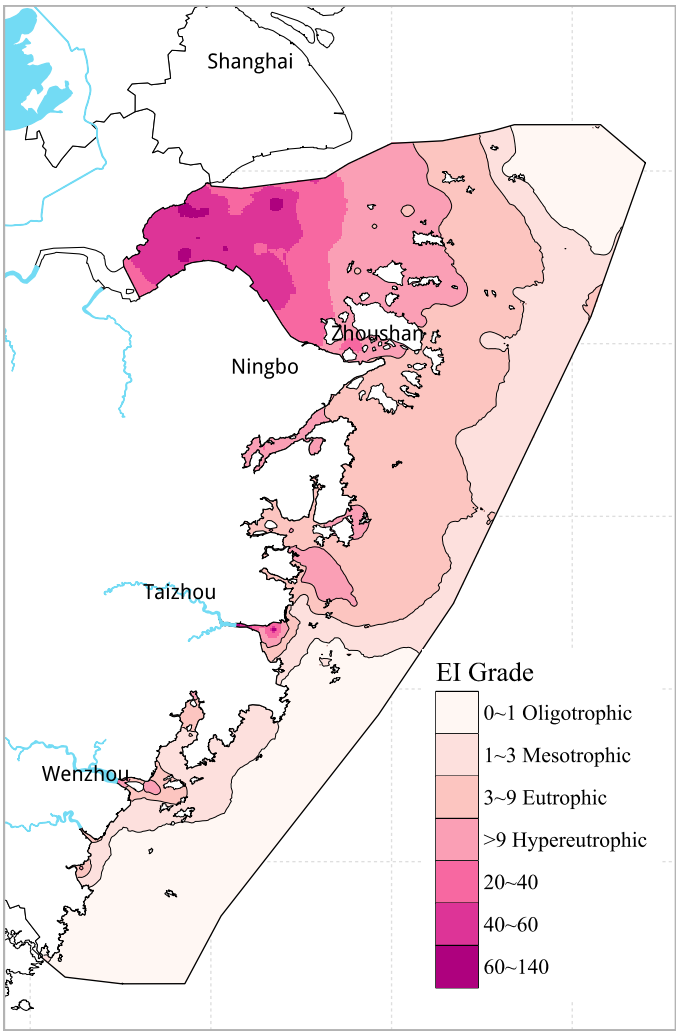

Fig. 4. Spatial map of eutrophication index (EI) distribution in the study region.

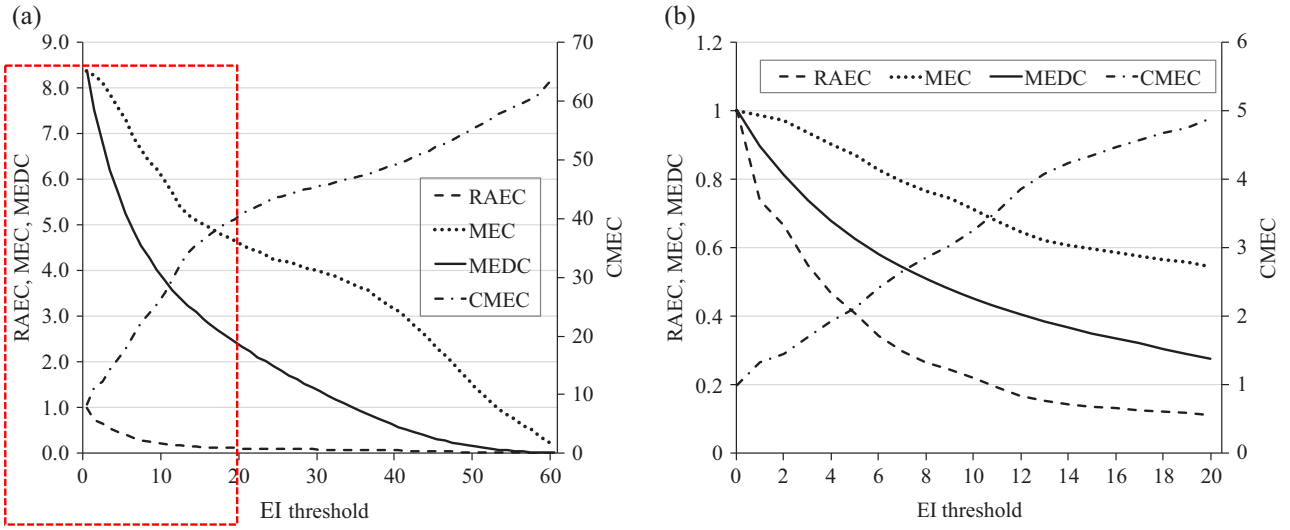

Fig. 5. (**a**) One-point SSI (RAEC, MEC, MEDC, and CMEC) in the Zhejiang coastal waters as functions of the eutrophication index threshold ζ. (**b**) Is a detailed plot of section $\zeta < 20$ of the red box of plot (**a**); in plot (**b**) the MEC, MEDC, and CMEC are normalized by the mean eutrophication index value, $\overline{\mathrm{EI}}$.

measures of excess marine contamination). Specifically, the following sections.

The RAEC of Zhejiang coastal waters eutrophication

The RAEC indicator, $R_{\mathrm{EI}}(\zeta)$, measures the ratio of eutrophicated water body over the total area D of the Zhejiang coastal waters. Its plot in Fig. 5a describes the fast decrease of the size of the coastal water area in which the EI exceeded the ζ threshold (i.e., EI > ζ) as a function of ζ. RAEC varies between 0 and 1. For $\zeta = 3.5$, it is found that RAEC = 0.5, indicating that in half of the coastal area, the eutrophication index is higher than 3.5. In other words, 3.5 is the median eutrophication index value in the study region. In addition, when $\zeta = 20$, it is found that RAEC = 0.11, which indicates that the EI values are less than 20 in about 9/10 of the coastal area (i.e., 1-RAEC = 0.89 ≈ 0.9).

The MEDC of Zhejiang coastal waters eutrophication

The MEDC indicator $L_{\mathrm{EI}}^{D}(\zeta)$ measures the spatial average of the difference between excess EI($\boldsymbol{s}$) and ζ (i.e., EI($\boldsymbol{s}$) − ζ) over the entire area D of the Zhejiang coastal waters. Its plot in Fig. 5a is a convex and decreasing function of the eutrophication threshold ζ; and the MEDC range is between 0 (at the maximum ζ value) and the $\overline{\mathrm{EI}} = 8.38$ (at $\zeta = 0$). MEDC decreases slower than RAEC as a function of ζ, implying that with increasing ζ the differential eutrophication value over the contaminated subregion of the Zhejiang coastal waters decreases slower than the area of the same subregion (which makes it possible that disproportionally large eutrophication values may exist in very small areas).

The MEC of Zhejiang coastal waters eutrophication

The MEC indicator $P_{\mathrm{EI}}^{D}(\zeta)$ of the Zhejiang coastal waters offers a global assessment of the expected over contamination in the fraction of the coastal region D where the eutrophication index exceeds the threshold ζ. The MEC plot in Fig. 5a is a positive, continuous and decreasing function of ζ. It starts at MEC = 8.38, meaning that the mean eutrophication index value in the study region is equal to 8.38. Just as MEDC, the MEC range is between zero (at the maximum ζ) and $\overline{\mathrm{EI}} = 8.38$ (at $\zeta = 0$), but MEC decrease slower than both MEDC and RAEC.

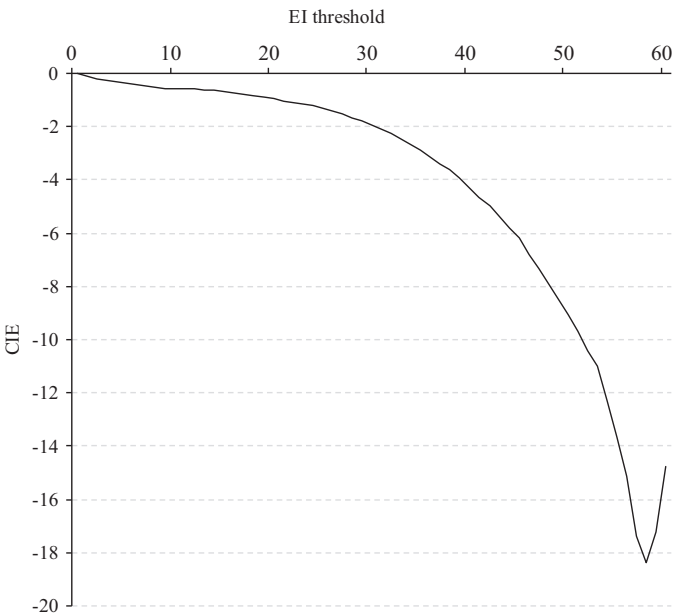

Fig. 6. Plot of the contaminant indicator elasticity (CIE) of MEDC, $Q_{L_{\mathrm{EI}}^{D}}$.

The CMEC of Zhejiang coastal waters eutrophication

On the contrary, the CMEC indicator $P_{\mathrm{EI}}^{\Theta}(\zeta)$ is an increasing function of ζ, since it measures the average of regional eutrophication index values exceeding threshold ζ. We recall that Θ was defined in Table 1 as the substantially contaminated subregion of the entire coastal region D. In this context, the CMEC is concerned with the contaminated coastal subregion Θ, whereas the MEC refers to the entire coastal region D. When $\zeta < 20$, the CMEC increased approximately linearly with threshold ζ (Fig. 5b), and when $\zeta > 20$, the increasing became flatter than before.

The CID of Zhejiang coastal waters eutrophication

The CID indicator Ψ_{EI} is the ratio of excess eutrophication dispersion over the mean EI($\boldsymbol{s}$). In the case of the Zhejiang coastal waters it was found that CID = 0.24, indicating that the average excess EI($\boldsymbol{s}$) dispersion is a small percentage of the mean eutrophication index.

The CIE of Zhejiang coastal waters eutrophication

An additional characterization of the eutrophication status is obtained by the elasticity of the MEDC indicator $L_{\mathrm{EI}}^{D}(\zeta)$ with respect to threshold ζ, i.e., CIE is a measure of the effect on MEDC of changes in ζ (when all other factors that affect MEDC are unchanged). The CIE can be expressed as.

$$Q_{L_{\mathrm{EI}}^{D}}(\zeta) = -\frac{R_{\mathrm{EI}}(\zeta)}{L_{\mathrm{EI}}^{D}(\zeta)}\zeta = -\frac{\zeta}{P_{\mathrm{EI}}^{\Theta}(\zeta)-\zeta}, \tag{7}$$

which means that the ζ-elasticity of MEDC is negative (i.e., a MEDC increase of, say, −5% is a positive MEDC decrease of 5%). The elasticity $Q_{L_{\mathrm{EI}}^{D}}(\zeta)$ is proportional to ζ with the proportionality coefficient being equal to the ratio $-\frac{\mathrm{RAEC}}{\mathrm{MEDC}}$ or, equivalently, the ratio $-\frac{1}{\mathrm{CMEC}-\mathrm{Threshold}}$. Accordingly, in practice the CIE can be computed either from the previously calculated RAEC and MEDC indicators or directly from the previously calculated CMEC indicator.

The elasticity of the MEDC indicator is plotted in Fig. 6 as a function of the eutrophication threshold ζ. It can be observed that: (1) As the ζ increases, the MEDC elasticity increases negatively (i.e., the MEDC decreases in magnitude). (2) Elasticity shows a peak at $\zeta \approx 55$, and starts dropping toward zero after that. (3) The larger the MEDC elasticity is, the more sensitive the eutrophication is to ζ changes (the elasticity plot starts from a zero value, i.e., $Q_{L_{\mathrm{EI}}^{D}} = 0$ when $\zeta = 0$, and increases exponentially with ζ). (4) In the CMEC plot of Fig. 5a, we noticed that $P_{\mathrm{EI}}^{\Theta}(\zeta) > \zeta$, which implies that $Q_{L_{\mathrm{EI}}^{D}} < 0$. This is, indeed, confirmed in the CIE plot of Fig. 6 (MEDC elasticity keeps decreasing up to $\zeta = 57$, and then starts increasing).

Two-point SSI

The two-point SSI of the present Zhejiang coastal waters study are plotted in Fig. 7a–c. It is noticed that the NIC, CIC, and CIR indicators exhibit decreasing trends with increasing threshold ζ (a similar discussion regarding the NEC, CEC and EDC indicators is presented in the Supporting Information section and Figs. 3–5). Specifically, the following sections.

The NIC of Zhejiang coastal waters eutrophication

The NIC is a bivariate eutrophication indicator, $c_1(\delta\mathbf{s}; \zeta)$, that depends on both the separation distance $\delta\mathbf{s}$ between any two locations in the Zhejiang coastal waters and on the eutrophication threshold ζ. As is shown in Fig. 7a, the regional NIC decreases significantly with increasing ζ, implying that the probability of threshold-exceeding eutrophication (i.e., EI($\boldsymbol{s}$) > ζ) at both coastal locations separated by $\delta\mathbf{s}$ decreases with increasing ζ. For smaller ζ values, the NIC is high, indicating a stronger threshold-exceeding eutrophication correlation across space, i.e., a stronger connectivity exists between the incidences "EI($\boldsymbol{s}$) > ζ at location $\mathbf{s}$" and "EI($\boldsymbol{s} + \delta\mathbf{s}$) > ζ at location $\mathbf{s} + \delta\mathbf{s}$". For numerical illustration, when the values of the

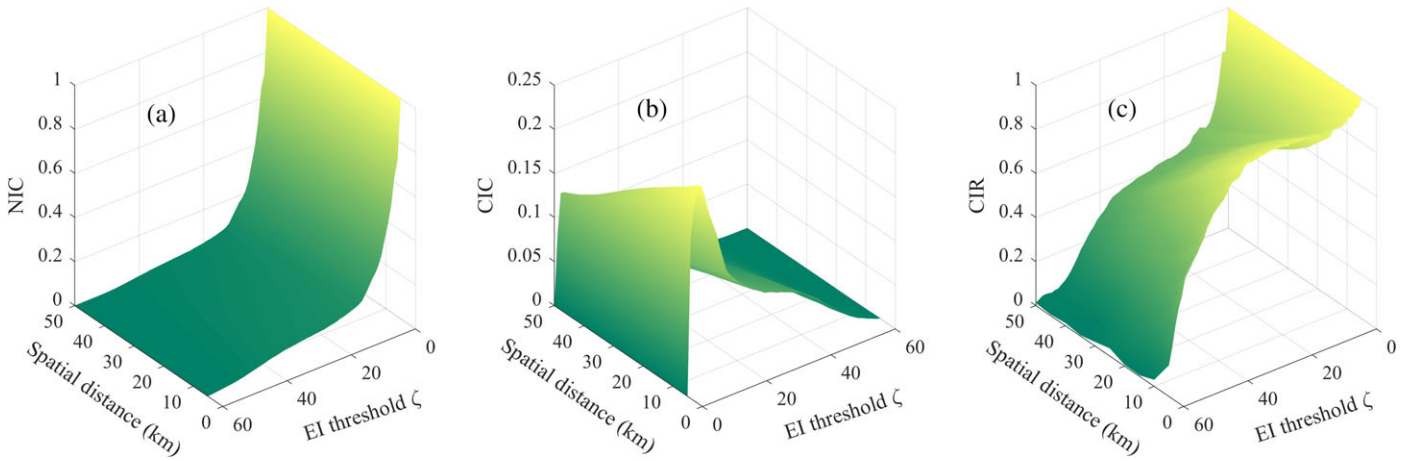

Fig. 7. (**a**–**c**) Plots of the NIC, CIC, and IR indicators in the Zhejiang coastal waters as functions of the EI threshold and the spatial distance between locations.

threshold ζ are equal to 1, 3, and 9, the corresponding mean NIC eutrophication values (probabilities) at spatial lags 5–50 km are 0.71, 0.51, and 0.19, respectively (alternative, these numbers may be interpreted as the probabilities that the eutrophication level does not cross the threshold ζ when it moves from coastal location $\mathbf{s}$ to $\mathbf{s} + \delta\mathbf{s}$; or, as the corresponding probabilities that both locations $\mathbf{s}$ and $\mathbf{s} + \delta\mathbf{s}$ fall within the contaminated subregion of the Zhejiang coastal waters). The ecological interpretation of this finding is of significant consequence: it implies that 71%, 51%, and 19% of the locations of the Zhejiang coastal waters separated by these spatial lags experience mesotrophic, eutrophic, and hypereutrophic risks, respectively. In addition, when the threshold $\zeta > 20$, the eutrophication NIC shows a rather slow decrease with increasing distance, indicating that, for this threshold range, the distance between any two coastal locations has little effect on the corresponding NIC value.

The CIC of Zhejiang coastal waters eutrophication

The CIC indicator, $\widetilde{c}_{\mathrm{I}}(\delta\mathbf{s};\zeta)$, measures the strength of threshold-exceeding eutrophication dependency in the Zhejiang coastal waters in terms of the magnitude of the quantity.

$$P[\mathrm{EI}(\boldsymbol{s}) > \zeta \text{ and } \mathrm{EI}(\boldsymbol{s}+\delta\boldsymbol{s}) > \zeta] - P[\mathrm{EI}(\boldsymbol{s}) > \zeta]P[\mathrm{EI}(\boldsymbol{s}+\delta\boldsymbol{s}) > \zeta].$$

Since the CIC value is non-negative for all thresholds and separation lags considered (*see*, Fig. 7b), the eutrophication dependency in the Zhejiang coastal waters is characterized as PQED (i.e., ζ-exceeding eutrophication incidences are probabilistically associated with other ζ-exceeding incidences). Also, when the ζ value is approaching the maximum or the minimum EI value, the regional CIC indicator tends to 0. The ecological meaning of this result is that for very large thresholds the spatial eutrophication dependency, as defined above, becomes negligible, and the incidences "EI($\boldsymbol{s}$) > ζ" and "EI($\boldsymbol{s}$ + $\delta\mathbf{s}$) > ζ" may be considered as independent from each other. On the other hand, it is worth noticing that when $\zeta \approx 8.38$ (i.e., the selected threshold is equal to the mean EI value over the Zhejiang coastal waters), the CIC indicator calculated at various spatial lags consistently reach its maximum value. The interpretation of this result is that the strongest eutrophication dependency occurs when $\zeta \approx 8.38$. Otherwise said, if $\zeta \approx 8.38$ is used to divided the Zhejiang coastal waters region into contaminated and noncontaminated subregions, the corresponding polygons will be more fragmentized than those divided based on other ζ values.

The $\zeta \approx 8.38$ is also a critical value in the sense that for $\zeta < 8.38$, the CIC indicator increases with ζ, implying that the eutrophication dependency between any locations separated by a certain distance $\delta\mathbf{s}$ increases as a function of ζ; whereas for $\zeta > 8.38$ the opposite is true, i.e., the CIC indicator deceases with ζ, implying that the eutrophication dependency between any locations separated by $\delta\mathbf{s}$ decreases withζ. Last, for any given ζ-value the CIC decreases with $\delta\mathbf{s}$, implying that eutrophication dependency between any locations separated by $\delta\mathbf{s}$ decreases with $\delta\mathbf{s}$.

Table 4. Water quality grades wth corresponding one-point SSI values, and two-point SSI values between locations at $\delta\mathbf{s}$ = 10 km distance apart.

ζ	0	1	3	9	60
RAEC	1	0.7405	0.5487	0.2456	0.0029
MEC	8.3784	8.2483	7.8356	6.2216	0.1882
MEDC	8.3784	7.5078	6.1896	4.0115	0.0119
CMEC	8.3784	11.1390	14.2807	25.3365	64.0597
CIE(MEDC)	0	−0.0986	−0.2659	−0.5509	−14.7795
NIC	1	0.7188	0.5210	0.2189	0.0002
CIC	0	0.1692	0.2138	0.1617	0.0001
CIR	1	0.9410	0.8868	0.8378	0.0292
Grade	Oligotrophic				
		Mesotrophic			
				Eutrophic	
					Hypereutrophic

The CIR of Zhejiang coastal waters eutrophication

The CIR indicator, $G_{\mathrm{EI}}(\delta\mathbf{s}, \zeta)$, introduces a comparative relationship between the probability that the EI exceeds the selected eutrophication threshold ζ at both locations separated by the distance $\delta\mathbf{s}$ within the Zhejiang coastal waters region, on the one hand, and the probability that EI exceeds the threshold ζ at either one of these two locations, on the other. More specifically, the CIR calculates what percentage of the "either-or" probability P[either EI($\boldsymbol{s}$) > ζ or EI($\boldsymbol{s}$ + $\delta\boldsymbol{s}$) > ζ] is the "and" probability P[EI($\boldsymbol{s}$) > ζ and EI($\boldsymbol{s}$ + $\delta\boldsymbol{s}$) > ζ] (recall that CIR ≤ 100% or 1). As is shown in Fig. 7c, the CIR decreases from its maximum value (equal to 1) as a function of the threshold ζ. This means that the larger the selected eutrophication threshold is, the smaller the fraction of the "either-or" eutrophication probability that belongs to the "both" probability. However, at distances smaller than the critical distance $\delta\mathbf{s}_{\mathrm{cr}} \approx 15$ km, the CIR value remains large (this observation holds even if the selected threshold is large), indicating that the locations with high EI values are concentrated in the coastal waters of the Zhejiang province rather than being dispersed.

Eutrophication mechanisms and management in the Zhejiang coastal waters

The coastal zone of Zhejiang province is densely populated and has China's biggest fishery (particularly, in the Zhoushan island waters), which may worsen water contamination due to industrial point sources and agricultural nonpoint sources. This coastal zone has suffered from considerable anthropogenic influences in recent decades. With abundant nutrients (such as N and P) discharged into Hangzhou Bay and the East China Sea by point or nonpoint source contamination, the study area has the highest frequency of red tides in China (Liu et al. 2013). Aquatic eutrophication directly leads to rapid

increase of algal biomass, which can cause not only reductions in dissolved oxygen levels, but also accumulations of toxic metabolites (Conley et al. 2009; Xiao et al. 2017). Consequently, the deterioration of water quality will damage the marine ecosystems, prevent recovery of fish stocks and threaten public health. The spatial spread of aquatic eutrophication directly leads to rapid increases of algal biomass that covers aquatic organisms and plants, thus reducing water transmittance and hindering the photosynthesis of the plants. Accordingly, this process can cause reductions in dissolved oxygen levels, as well as accumulations of toxic metabolites in seawater (Conley et al. 2009; Xiao et al. 2017).

Nitrogen and phosphorus concentrations in the Zhejiang coastal waters severely exceeded the regional standards (note that SSI were also calculated for N and P, *see* Supporting Information Figs. 6–S8). This situation was caused by large amounts of nutrients from freshwater and anthropogenic impacts, such as industrial activities, transport, and tourism. About 43.06% and 32.6% of the coastal waters exceeded the 4^{th} grade standard for nitrogen concentration (0.5 mg/L) and phosphorous (0.045 mg/L), respectively. The average eutrophication index is 8.38, which is much larger than 3, indicating severe eutrophication in the region. Those high values are mainly found around estuaries, especially Hangzhou Bay, where large amount of nutrients come from freshwater runoff.

For water quality management purposes, some interesting observations can be made based on Table 4, as follows:

i. Based on the RAEC values of Table 4, it is inferred that in 75.05% of the Zhejiang coastal waters the water quality grade is oligotrophic or higher, in 54.87% the grade is eutrophic or higher, and in 24.56% the grade is hypereutrophic).
ii. By calculating the RAEC differences for the thresholds 1, 3, and 9 of the EI classification standards ("Eutrophication index" section above), it is found that in 25.95% of the Zhejiang coastal waters the quality grade is oligotrophic, in 19.18% mesotrophic, in 30.31% eutrophic, and in 24.17% hypereutrophic. Interestingly, these numbers coincide with the corresponding area percentages of the EI map in Fig. 4 (see, also, discussion in "Eutrophication assessment and classification maps" section above), a fact that further confirms the validity of the RAEC-based results.
iii. From the MEC values of Table 4, we find that the average EI over the Zhejiang coastal waters region is 8.3784, and the $EI > 1$, $EI > 3$, and $EI > 9$ values averaged over the same region are 8.2483, 7.8356, and 6.2216, respectively.
iv. Based on the CMEC values, it is concluded that the average EI value over the subregion of the Zhejiang coastal waters graded as "oligotrophic or higher" is 11.139, the average EI over the subregion graded as "eutrophic or higher" is 14.2807, and the average EI over the subregion graded as "hypereutrophic" is 25.3365.
v. The MEDC values indicate that the average EI-1, EI-3, and EI-9 values over the Zhejiang coastal waters region are, respectively, 7.5078, 6.1896, and 4.0115. Remarkably, the elasticity of the MEDC indicator is several times larger for the eutrophic grade than for the oligotrophic and mesotrophic grades (compare, e.g., CIE = –0.5509 vs. –0.0986 and – 0.2659).
vi. Based on the NIC values of Table 4, the probability of threshold-exceeding EI at both coastal locations separated by, say, $\delta\mathbf{s}$ = 10 km is higher in the oligotrophic subregion, and then reduces gradually as we move to the mesotrophic, then to the eutrophic and, finally, to the hypereutrophic domains.
vii. The CIC values indicate that EI dependency between pairs of locations (PQED) increases as we move from the oligotrophic to the mesotrophic domain, and then reduces as we move to the eutrophic and hypereutrophic domains.
viii. The CIR values imply that the ratio of the "and" EI dependence probability over the "either-or" dependence probability is higher in the oligotrophic domain, and then reduces gradually as we move to the mesotrophic, then to the eutrophic and, finally, to the hypereutrophic domains.

For the ecological remediation of eutrophication in the coastal waters of Zhejiang province, the effective management of anthropogenic activities is currently considered a feasible approach for reducing the N and P input (in this respect, the findings and results of this work, including the EI classification map of Fig. 4 and the numerical results of Table 4, may be useful for management purposes). A more extensive monitoring of the region is needed for a continuously improving water contamination assessment.

Conclusions

In this study, the eutrophication status and changing trend of the Zhejiang coastal waters were characterized quantitatively based on seawater quality monitoring data during August 2015. Overall, it was found that this region experiences severe eutrophication, especially inside the Hangzhou Bay. The main reasons for eutrophication include excessive nutrient loading into coastal waters, intense human activities, and low environmental protection awareness.

We used the BME technique for water quality maps and stochastic site indicators for the subsequent eutrophication assessment and characterization of the Zhejiang coastal waters region. Based on its ability to account for in situ uncertainty and assimilate different information sources without making restrictive modeling assumptions, BME generated the most accurate and informative maps of water quality attributes compared to the mainstream IDW and OK techniques. Specifically, the cross-validation results showed that BME generated water quality maps (COD, DIN, and DIP) with the smallest MAE and RMSE values compared to the other two techniques. Based on the BME maps, an eutrophication index (EI) was

adopted for further water quality assessment. The results showed that about 25.95%, 19.18%, 20.53%, and 34.34% of the coastal waters in Zhejiang Province were oligotrophic, mesotrophic, eutrophic, and hypereutrophic, respectively. That is, more than half of the marine water areas were in serious eutrophication status and showed a decreasing trend from estuary to open sea.

Moreover, the one-point and two-point stochastic site indicators were used to improve eutrophication characterization in the Zhejiang coastal waters. Specifically, the RAEC, MEC, and MEDC indicators decreased sharply for threshold ζ values below 20, whereas the CMEC indicator showed an approximately linearly increase as a function of ζ. For $\zeta = 3.5$ it was found that RAEC = 0.5, indicating that in half of the study region the EI was larger than 3.5. And when the ζ values are equal to 1, 3, and 9, the NIC values at various spatial lags are equal to 0.71, 0.51, and 0.19, respectively, indicating that 71%, 51%, and 19% of location pairs separated by these lags experience mesotrophic, eutrophic, and hypereutrophic risks, respectively. The CIC indicator values designate that the contamination status of the Zhejiang coastal waters is characterized by its positive quadrant eutrophication dependency (i.e., the strength of joint eutrophication between any two coastal locations is consistently greater than the combined strength of independent eutrophications at these locations). In fact, a critical eutrophication threshold $\zeta_{cr} \approx 8.38$ exists for the Zhejiang coastal waters region such that for $\zeta < \zeta_{cr}$ the spatial eutrophication dependency increases with ζ, whereas for thresholds above $\zeta > \zeta_{cr}$ the opposite is true. Moreover, spatial eutrophication dependency decreases with separation distance $\delta\mathbf{s}$, and a critical distance $\delta\mathbf{s}_{cr} \approx 15$ km was determined for $\delta\mathbf{s} < \delta\mathbf{s}_{cr}$ the excess eutrophication locations are concentrated in the coastal waters of the Zhejiang province rather than being dispersed.

Elasticity analysis of the eutrophication MEDC indicator provided a useful measure of the mean excess eutrophication change in Zhejiang coastal waters caused by an environmental threshold change. In this context, it was found that the larger the elasticity of the eutrophication MEDC indicator is, the more sensitive eutrophication is to threshold changes. Eutrophication control measures of the Zhejiang coastal waters are strongly suggested, such as combining pollutant source control (e.g., reducing the amount of nutrients and controlling endogenous contamination) with ecological restoration (e.g., coastal zone formation and protection), and regulatory management of human activities.

References

Chen, C. W., Y. R. Ju, C. F. Chen, and C. D. Dong. 2016. Evaluation of organic pollution and eutrophication status of Kaohsiung Harbor, Taiwan. Int. Biodeterior. Biodegradation **113**: 318–324. doi:10.1016/j.ibiod.2016.03.024

Christakos, G. 1990. A Bayesian maximum-entropy view to the spatial estimation problem. Math. Geol. **22**: 763–777. doi:10.1007/BF00890661

Christakos, G. 2000. Modern spatiotemporal geostatistics. Oxford Univ. Press.

Christakos, G., and D. T. Hristopulos. 1996*a*. Characterization of atmospheric pollution by means of stochastic indicator parameters. Atmos. Environ. **30**: 3811–3823. doi:10.1016/1352-2310(96)00083-0

Christakos, G., and D. T. Hristopulos. 1996*b*. Stochastic indicators for waste site characterization. Water Resour. Res. **32**: 2563–2578.

Christakos, G., and D. T. Hristopulos. 1997. Stochastic indictor analysis of contaminated sites. J. Appl. Probab. **34**: 988–1008. doi:10.2307/3215012

Conley, D. J., H. W. Paerl, R. W. Howarth, D. F. Boesch, S. P. Seitzinger, K. E. Havens, C. Lancelot, and G. E. Likens. 2009. Ecology. Controlling eutrophication: nitrogen and phosphorus. Science **323**: 1014. doi:10.1126/science.1167755

Coulliette, A. D., E. S. Money, M. L. Serre, and R. T. Noble. 2009. Space/time analysis of fecal pollution and rainfall in an eastern North Carolina estuary. Environ. Sci. Technol. **43**: 3728–3735. doi:10.1021/es803183f

He, J., and A. Kolovos. 2017. Bayesian maximum entropy approach and its applications: A review. Stoch. Environ. Res. Risk Assess. **6**: 1–19.

Heip, C. 1995. Eutrophication and zoobenthos dynamics. Ophelia **41**: 113–136.

Howarth, R. W., and R. Marino. 2006. Nitrogen as the limiting nutrient for eutrophication in coastal marine ecosystems: Evolving views over three decades. Limnol. Oceanogr. **51**: 364–376. doi:10.4319/lo.2006.51.1_part_2.0364

Hutchinson, G. E. 1967. A treatise on limnology. Introduction to lake biology and the limnoplankton, v. **v. II**. John Wiley & Sons.

Kitsiou, D., and M. Karydis. 2000. Categorical mapping of marine eutrophication based on ecological indics. Sci. Total Environ. **255**: 113–127.

Kong, X., Y. Sun, R. Su, and X. Shi. 2017. Real-time eutrophication status evaluation of coastal waters using support vector machine with grid search algorithm. Mar. Pollut. Bull. **119**: 307–319. doi:10.1016/j.marpolbul.2017.04.022

Siu-Nganlam, N. 1983. Spatial interpolation methods: A review. The American Cartographer **10**: 129–150.

Liu, L., J. Zhou, B. Zheng, W. Cai, K. Lin, and J. Tang. 2013. Temporal and spatial distribution of red tide outbreaks in the Yangtze River Estuary and adjacent waters, China. Mar. Pollut. Bull. **72**: 213–221. doi:10.1016/j.marpolbul.2013.04.002

Liu, R. M., Y. X. Chen, C. C. Sun, P. P. Zhang, J. W. Wang, W. W. Yu, and Z. Y. Shen. 2014. Uncertainty analysis of total phosphorous spatial-temporal variations in the Yangtze river estuary using different interpolation methods. Mar. Pollut. Bull. **86**: 68–75. doi:10.1016/j.marpolbul.2014.07.041

Liu, T. K., P. Chen, and H. Y. Chen. 2015. Comprehensive assessment of coastal eutrophication in Taiwan and its

implications for management strategy. Mar. Pollut. Bull. **97**: 440–450. doi:10.1016/j.marpolbul.2015.05.055

Lundberg, C., B. M. Jakobsson, and E. Bonsdorff. 2009. The spreading of eutrophication in the eastern coast of the Gulf of Bothnia, northern Baltic Sea—an analysis in time and space. Estuar. Coast Shelf Sci. **82**: 152–160. doi:10.1016/j.ecss.2009.01.005

Modis, K., K. I. Vatalis, and C. Sachanidis. 2013. Spatiotemporal risk assessment of soil pollution in a lignite mining region using a Bayesian maximum entropy (BME) approach. Int. J. Coal Geol. **112**: 173–179. doi:10.1016/j.coal.2012.11.015

Naumann, E. 1919. Nagra synpunkter angaende limnoplanktons okologi med sarskild hansyn till fytoplankton. Sven. Bot. Tidskr. **13**: 129–163.

Nikolaidis, G., D. P. Patoucheas, and K. Moschandreou. 2006. Estimating breakpoints of chl-a in relation with nutrients from Thermaikos Gulf (Greece) using piecewise linear regression. Fresen. Environ. Bull. **15**: 1189–1192.

Olea, R. A. 1999. Geostatistics for engineers and earth scientists. Kluwer.

Postma, H. 1966. The cycle of nitrogen in the Wadden Sea and adjacent areas. Neth. J. Sea Res. **3**: 186–221.

Primpas, I., G. Tsirtsis, M. Karydis, and G. D. Kokkoris. 2010. Principal component analysis: Development of a multivariate index for assessing eutrophication according to the European water framework directive. Ecol. Indic. **10**: 178–183. doi:10.1016/j.ecolind.2009.04.007

Quan, W. M., X. Q. Shen, and J. D. Han. 2005. Analysis and assessment on eutrophication status and developing trend in Changjiang Estuary and adjacent sea (in Chinese). Mar. Environ. Sci. **24**: 13–16.

Ren, J., B. B. Gao, H. M. Fan, Z. H. Zhang, Y. Zhang, and J. F. Wang. 2016. Assessment of pollutant mean concentrations in the Yangtze estuary based on msn theory. Mar. Pollut. Bull. **113**: 216. doi:10.1016/j.marpolbul.2016.09.021

Smith, V. H. 2006. Responses of estuarine and coastal marine phytoplankton to nitrogen and phosphorus enrichment. Limnol. Oceanogr. **51**: 377–384. doi:10.4319/lo.2006.51.1_part_2.0377

Vollenweider, R. A. 1992. Coastal marine eutrophication: Principles and control, p. 1–20. *In* R. A. Vollenweider, R. Marchetti, and R. Viviani [eds.], Marine coastal eutrophication. Elsevier.

Wang, J. F., X. H. Li, G. Christakos, Y. L. Liao, T. Zhang, X. Gu, and X. Y. Zheng. 2010. Geographical detectors-based health risk assessment and its application in the neural tube defects study of the Heshun region, China. Int. J. Geogr. Inf. Sci. **24**: 107–127. doi:10.1080/13658810802443457

Wang, J. F., T. L. Zhang, and B. J. Fu. 2016. A measure of spatial stratified heterogeneity. Ecol. Indic. **67**: 250–256. doi:10.1016/j.ecolind.2016.02.052

Xiao, X., and others 2017. A novel single-parameter approach for forecasting algal blooms. Water Res. **108**: 222–231. doi:10.1016/j.watres.2016.10.076

Xiao, Y., J. G. Ferreira, S. B. Bricker, J. P. Nunes, M. Zhu, and X. Zhang. 2007. Trophic assessment in Chinese coastal system-review of methods and application to the changjiang (Yangtze) estuary and Jiaozhou Bay. Estuaries Coast. **30**: 901–918. doi:10.1007/BF02841384

Yang, Y., and G. Christakos. 2015. Spatiotemporal characterization of ambient PM2.5 concentrations in Shandong province (China). Environ. Sci. Technol. **49**: 13431–13438. doi:10.1021/acs.est.5b03614

Yu, C. Y., and others. 2013. Study on eutrophication status and trend in Bohai Sea (in Chinese). Mar. Environ. Sci. **32**: 175–177.

Yu, H. L., A. Kolovos, G. Christakos, J. C. Chen, S. Warmerdam, and B. Dev. 2007. Interactive spatiotemporal modeling of health systems: The SEKS-GUI framework. Stoch. Environ. Res. Risk Assess. **21**: 555–572. doi:10.1007/s00477-007-0135-0

Yu, H. L., C. H. Wang, M. C. Liu, and Y. M. Kuo. 2011. Estimation of fine particulate matter in Taipei using land use regression and Bayesian maximum entropy methods. Int. J. Environ. Res. Public Health **8**: 2153–2169. doi:10.3390/ijerph8062153

Zhang, F., X. Sun, Y. Zhou, C. Zhao, Z. Du, and R. Y. Liu. 2017. Ecosystem health assessment in coastal waters by considering spatio-temporal variations with intense anthropogenic disturbance. Environ. Model. Softw. **96**: 128–139. doi:10.1016/j.envsoft.2017.06.052

Acknowledgments

This research was supported by the National Science Foundation of China (Grant No. 41671399) and the China Scholarship Council (201706320278).

Conflict of Interest

None declared.

Submitted 14 November 2017
Revised 5 May 2018
Accepted 29 June 2018

Associate editor: Josette Garnier